

Measurement of Neutrons Produced by Inertial Fusion with a Diamond Radiation Detector

Takehiro Shimaoka,¹ Junichi H. Kaneko,^{1*} Yasunobu Arikawa,² Mitsutaka Isobe,³
Masakatsu Tsubota,¹ Kengo Oda,¹ Mitsuo Nakai,² Hiroyuki Shiraga,²
Hiroshi Azechi,² Akiyoshi Chayahara,⁴ Hitoshi Umezawa,⁴ and Shinichi Shikata⁴

¹Graduate School of Engineering, Hokkaido University,
Kita 13 Nishi 8, Kita-ku, Sapporo, Hokkaido 060-8628, Japan

²Osaka University, 2-6 Yamada-oka, Suita, Osaka 565-0871, Japan

³National Institute for Fusion Science, 322-6 Oroshi-cho, Toki, Gifu 509-5292, Japan

⁴Diamond Research Laboratory, National Institute of Advanced Industrial Science and Technology (AIST),
1-8-31 Midorigaoka, Ikeda, Osaka 563-8577, Japan

(Received September 28, 2023; accepted January 5, 2024)

Keywords: diamond, radiation detector, ICF, neutron, bang monitor

We evaluated the neutron bang time in fast-ignition inertial confinement fusion and the response function of deuterium-deuterium (DD) neutrons for burn history monitoring applications with a single-crystal CVD diamond detector. Signals were successfully obtained for the first time with a single-crystal diamond detector for DD neutrons of above 10^8 neutrons/shot.

1. Introduction

A fast ignition method, which is an evolution of the direct irradiation method, is being developed to improve the fusion gain in inertial confinement fusion experiments.⁽¹⁾ At Osaka University, a target with a gold cone attached to a fuel sphere is used, and the high-temperature, high-density plasma formed by direct irradiation is irradiated by laser for the first ignition experiment (LFEX) with an energy of 1 kJ and a time width of 1 ps. As a result, the plasma is heated by fast electrons generated from the gold cone, and fusion ignition is expected to be achieved at about one-tenth the energy of that in the direct irradiation method.

For the optimization of fast ignition, it is important to know the implosion instability, the core plasma behavior, the dynamics of heating by fast electrons, the neutron production dynamics, and so forth. To obtain such information, plasma diagnostics using nuclear reaction particle measurement^(2,3) and X-ray spectroscopic imaging^(4,5) have been attempted. Among the parameters obtained by plasma diagnostics, the neutron bang time, which indicates the peak time of neutron production, and the neutron burn history, which reveals the time variation of the neutron production history, are indices related to neutron

*Corresponding author: e-mail: higedon@eng.hokudai.ac.jp
<https://doi.org/10.18494/SAM4671>

production dynamics. Detectors capable of measuring these parameters with a time resolution of better than 100 ps are required.

At the National Ignition Facility (NIF), neutron bang time measurements using fast plastic scintillators⁽⁶⁾ and polycrystalline CVD diamond⁽⁷⁾ detectors have been reported. Neutron burn history measurements with a time resolution of 10 ps using an X-ray streak camera have also been reported.⁽⁸⁾

On the other hand, the above measurements have not been successful for the fast ignition method. There are two reasons for this. The first is that the total number of neutrons is small. In the fast ignition method at Osaka University, the energy input is smaller than that at the NIF, and the deuterium-deuterium (DD) fuel sphere, which has a small nuclear reaction cross section, is used for implosion. The total number of neutrons produced was about 10^7 – 10^8 , less than 1/1000 of that of the NIF. The second is that bremsstrahlung X-rays are generated by fast electrons. Bremsstrahlung X-rays with a maximum energy on the order of 10 MeV are generated at 10^{12} – 10^{15} photons/shot, and when plastic scintillators are used, afterglow with a decay time of μ s order and afterpulses from the photomultiplier tubes are generated, making neutron measurement difficult.^(9,10)

To solve these problems, we have focused on and developed a single-crystal diamond detector as a neutron bang time and neutron burn history detector that can be used under the high X-ray intensity associated with fast ignition. Compared with polycrystalline diamond detectors, single-crystal diamond detectors have superior charge collection efficiency. Since there is no influence of charge capture by grain boundaries, the amount of charge detected per volume can be improved, and detailed neutron yield evaluation can be expected due to the reduced variation in the amount of charge. So far, single-crystal diamond detectors have shown a good response to X-rays generated by fast ignition with a half width of 0.8 ns and no afterpulse. However, owing to insufficient neutron sensitivity and electromagnetic noise, we have not succeeded in observing the neutron signal.⁽¹¹⁾ In this study, the entire measurement system including the power supply was installed in an electromagnetic shield, and the trigger signal was transmitted through an optical fiber. The system was electrically floated to reduce the noise level, and we attempted to detect neutrons.

2. Materials and Methods

2.1 Sample preparation

Single-crystal diamond was grown homoepitaxially on an off-angle-controlled high pressure/high temperature (HP/HT) Ila-type substrate using a microwave plasma CVD system (5250; ASTeX). The growth conditions were a gas pressure of 110 Torr, a substrate temperature of 850 °C, a microwave power of 1000 W, and a $\text{CH}_4/[\text{H}_2+\text{CH}_4]$ concentration of 0.25%. The grown layer was lifted off by electrolytic etching⁽¹²⁾ to obtain a freestanding film with an area of $5 \times 5 \text{ mm}^2$ and a thickness of 150 μm . An Al Schottky electrode of $\Phi 3 \text{ mm}$ and a thickness of 100 nm was fabricated on the as-grown surface by resistance heating deposition, and a TiC/Au ohmic

electrode with $\Phi 3$ mm and a thickness of 100 nm was fabricated on the substrate side surface by electron beam deposition. The former was grounded to an Al detector mount. The latter was wired to the subminiature type a (SMA) receptacle for high-voltage application and signal readout. The charge collection efficiency of the detector was evaluated by α -ray-induced charge distribution measurement. The charge collection efficiency for both electrons and holes was almost 100%. For details, please see Ref. 13.

2.2 DD neutron response function measurement system using GEKKO XII laser

We attempted to obtain the response function of a single-crystal diamond detector for DD neutrons generated by deuterium target implosion at the Laser Energetics Laboratory, Osaka University using the GEKKO XII laser. Figure 1 shows the measurement system. A bias tee (Picosecond Lab) with an analog frequency bandwidth of 16 GHz, a detector power supply (428; Ortec), and an oscilloscope (N2940A; Keysight) with an analog frequency bandwidth of 4 GHz and a sampling rate of 20 GS/s were used for the measurements. Inertial fusion devices generate strong electromagnetic noise due to laser irradiation, which makes it difficult to detect signals from the measurement target. Therefore, we fabricated an electrically floating measurement system from the detector to the measurement instrument as follows. The detector, coaxial cable, and measurement instrument were installed in a metalGS tube and a laboratory-made Cu

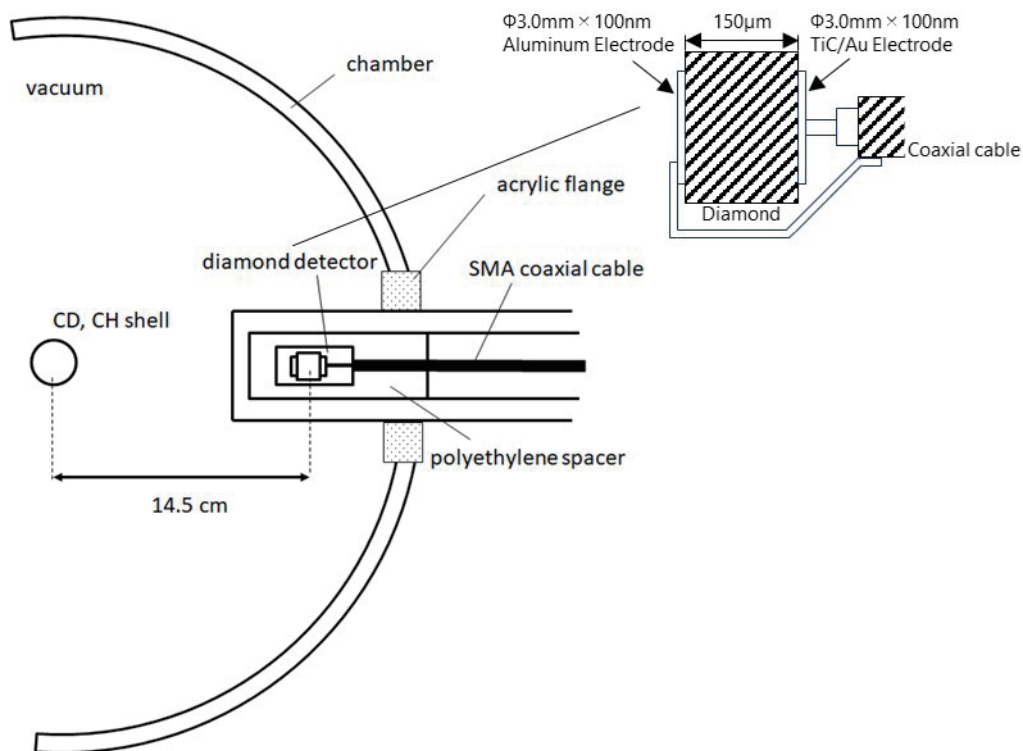


Fig. 1. Schematic drawing of DD neutron ToF measurement system based on a diamond radiation detector.

shielded box for electromagnetic shielding. The detector introduction port was insulated from the target chamber using an acrylic flange. The shielded box was placed on an insulating PTFE block, and the entire measurement system was electrically floated by using UPS battery power to drive the instruments. In addition, a trigger signal was introduced by an optical fiber and a photodiode (S5371; Hamamatsu).

The arrival time broadening due to the Doppler effect of DD neutrons is expressed as⁽¹⁴⁾

$$\Delta t \text{ (ps)} = 778 \times d \times \sqrt{T_i} \text{ (2.45 MeV DD neutron)}, \quad (1)$$

where T_i is the ion temperature (keV) and d is the distance between the target and the detector (m). Currently, the ion temperature for fast ignition in the FIREX project is about 0.5–1 keV.⁽¹⁵⁾ The detector must be placed within 5.7 cm from the target center to measure the time width of the 2.45 MeV neutrons produced by the DD reaction at an ion temperature of 5 keV after successful fast ignition in less than 100 ps. The photon and DD neutron velocities are 30 and 2.1 cm/ns, respectively; thus, the DD neutrons reach the detector 2.5 ns after the X-rays. The detector is required to have a fast response that can discriminate between photons and neutrons in time. In this measurement, the distance between the target and the detector was 14.5 cm owing to the combination of solid angles with other instruments.

To measure the DD neutron response function, a thin 2–3- μm -thick deuterium-gas-filled CD shell was used to increase the implosion rate and obtain a high neutron generation rate. The target implosion was performed only with the GEKKO XII laser, and the ToF method was used to detect the neutrons produced by the implosion. The expected number of DD neutrons was 10^8 neutrons/shot and the wave height value calculated from the detector sensitivity is a few mV, which is small. To confirm the presence of a neutron signal, we also compared the output signal with that of a deuterium-free CH shell explosion shot.

3. Experimental Results and Discussion

Figure 2 shows the response functions for CD and CH shell implosions. The electromagnetic noise was 2 mV peak-to-peak. The zero point of time in the figure corresponds to the rising edge of the photodiode. In the response functions of the CD shell implosions shown in Figs. 2(a)–2(c), X-ray and DD neutron signals from the imploding plasma were observed at -43 and -37 ns, respectively. The time difference between the X-ray and DD neutron signals is 6.2 ns, which corresponds to 14.5 cm between the target center and the detector. The neutron yield was calibrated with a plastic scintillator. The arrival time difference between X-ray and DD neutrons was constant, and an increase in wave height with increasing neutron yield was observed. Furthermore, as shown in Fig. 2(d), no neutron signal was observed for the CH-shell-only implosion. From these results, we confirmed that the pulse wave height at -37 ns is due to DD neutrons.

If the FIREX project progresses and the ion temperature of 5 keV is achieved, the total number of neutrons produced is expected to be 10^{11} neutrons/shot. As mentioned earlier, the distance between the detector and the target must be within 5.7 cm to measure neutrons with a time width of less than 100 ps. This detector has a neutron sensitivity of 2×10^{-8} mV/

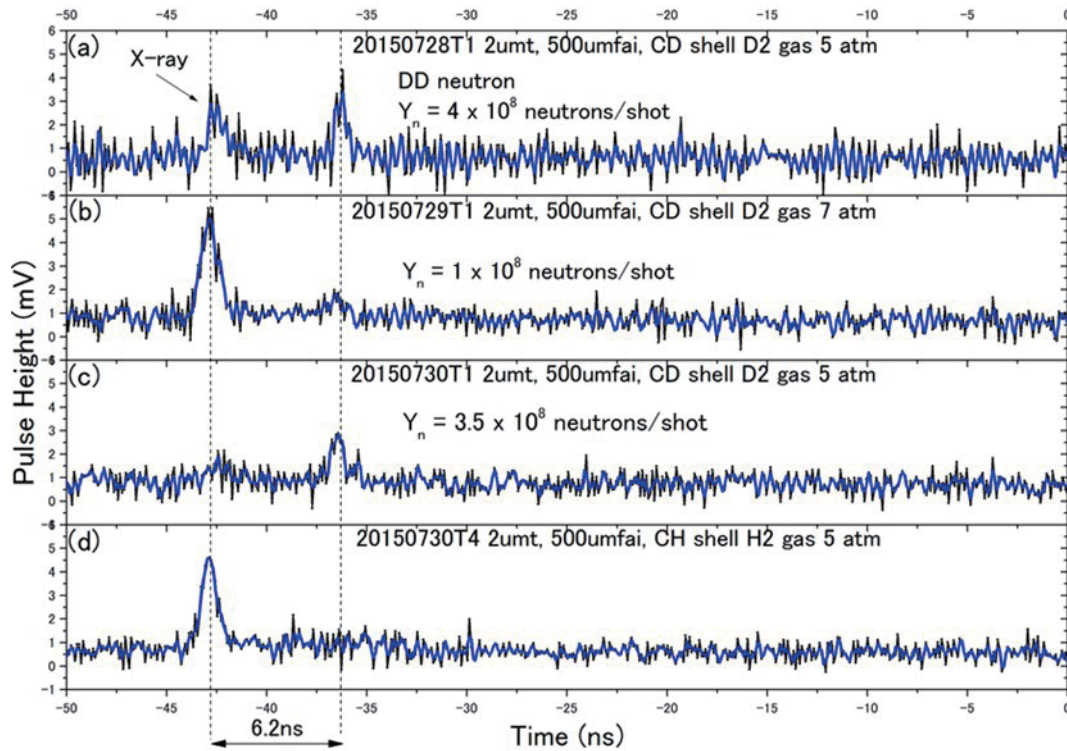


Fig. 2. (Color online) Examples of time responses of the diamond radiation detector for implosions of (a)–(c) CD(C_8D_8) shells and (d) CH (C_8H_8) shell. The blue lines show the five-point moving average.

neutrons in terms of the wave height for DD neutrons. If the neutron yield when fast ignition is achieved is $Y_n = 1 \times 10^{11}$ neutrons/shot and the wave height increases linearly with the number of neutrons, an output signal of 2 V can be expected. In the fast ignition system, electromagnetic noise is generated by the LFEX laser irradiation. Currently, the noise level in this measurement system is on the order of 10 to 100 mV. Furthermore, the X-ray signal intensity is expected to be a few volts, which is the same order of magnitude as the neutron signal intensity.

In neutron burn history measurement, electromagnetic noise and the overlap of X-ray and neutron signal wave heights cause measurement errors, because unfolding is performed on the acquired wave height values. To counter these problems, it is essential to further strengthen the electrostatic shielding and reduce the wave height of the X-ray signal by using a gate high-voltage mechanism. It is also important to increase the sensitivity of the diamond detector by increasing its area. Through the above efforts, we aim to realize the measurement of the neutron bang time and neutron burn history at the time of fast ignition.

4. Conclusion

The response function of a single-crystal CVD diamond detector to DD neutrons was evaluated. The applicability of this detector as a neutron burn history monitor and issues to be

resolved were discussed on the basis of the experimentally evaluated neutron sensitivity. In the evaluation of the response function for DD neutrons, we succeeded in obtaining signals at a neutron fluence of 10^8 neutrons/shot or higher for the first time by using electromagnetic shielding and electrical floating of the measurement system. Since there is no afterpulse, the diamond radiation detector can be expected to be effective for bang time and burn history measurement when the neutron yield is sufficient under intense X-ray conditions where photomultiplier tubes cannot be used at present.

Acknowledgments

This study was supported by Research Fellowships of the Japan Society for the Promotion of the Science for Young Scientists (Grant No. 13J02500).

References

- 1 M. Koga, Y. Arikawa, H. Azechi, Y. Fujimoto, S. Fujioka, H. Habara, Y. Hironaka, H. Homma, H. Hosoda, T. Jitsuno, T. Johzaki, J. Kawanaka, R. Kodama, K. Mima, N. Miyanaga, M. Murakami, H. Nagatomo, M. Nakai, Y. Nakata, H. Nakamura, H. Nishimura, T. Norimatsu, Y. Sakawa, N. Sarukura, K. Shigemori, H. Shiraga, T. Shimizu, H. Takabe, M. Tanabe, K. A. Tanaka, T. Tanimoto, T. Tsubakimoto, T. Watari, A. Sunahara, M. Isobe, A. Iwamoto, T. Mito, O. Motojima, T. Ozaki, H. Sakagami, T. Taguchi, Y. Nakao, H. Cai, M. Key, P. Norreys, and J. Pasley: Nucl. Instrum. Methods Phys. Res., Sect. A **653** (2011) 84. <https://doi.org/10.1016/j.nima.2011.01.101>
- 2 N. Izumi, K. Yamaguchi, T. Yamagajo, T. Nakano, T. Kasai, T. Urano, H. Azechi, S. Nakai, and T. Iida: Rev. Sci. Instrum. **70** (1999) 1221. <https://doi.org/10.1063/1.1149430>
- 3 T. Nagai, Y. Ioka, A. Hasegawa, K. Wada, S. Takaoku, M. Takata, K. Noritake, Y. Minami, K. Watanabe, K. Yamanoi, Y. Arikawa, H. Hosoda, H. Nakamura, T. Watari, M. Cadatal-Raduban, M. Koga, T. Shimizu, N. Sarukura, H. Shiraga, M. Nakai, T. Norimatsu, and H. Azechi: Jpn. J. Appl. Phys. **50** (2011) 080208. <https://doi.org/10.1143/JJAP.50.080208>
- 4 M. Koga, T. Fujiwara, T. Sakaiya, M. Lee, K. Shigemori, H. Shiraga, and H. Azechi: Rev. Sci. Instrum. **79** (2008) 10E909. <https://doi.org/10.1063/1.2968105>
- 5 M. Heya, M. Nakasuji, H. Shiraga, N. Miyanaga, H. Azechi, H. Takabe, T. Yamanaka, and K. Mima: Rev. Sci. Instrum. **68** (1997) 820. <https://doi.org/10.1063/1.1147698>
- 6 R. A. Lerche, V. Y. Glebov, M. J. Moran, J. M. McNaney, J. D. Kilkenny, M. Eckart, R. A. Zacharias, J. J. Haslam, T. J. Clancy, M. F. Yeoman, D. P. Warwas, T. C. Sangster, C. Stoeckl, J. Knauer, and C. J. Horsfield: Rev. Sci. Instrum. **81** (2010) 10D319. <https://doi.org/10.1063/1.3478680>
- 7 M. A. Barrios, A. MacPhee, S. P. Regan, J. Kimbrough, S. R. Nagel, L. R. Benedetti, S. F. Khan, D. Bradley, P. Bell, D. Edgell, and G. W. Collins: Rev. Sci. Instrum. **83** (2012) 10E105. <https://doi.org/10.1063/1.4729667>
- 8 S. F. Khan, P. M. Bell, D. K. Bradley, S. R. Burns, J. R. Celeste, L. S. Dauffy, M. J. Eckart, M. Geissel, D. I. Headley, J. P. Holder, N. Izumi, M. C. Jones, J. W. Kellogg, H. Y. Khater, J. R. Kimbrough, A. G. MacPhee, Y. P. Opachich, N. E. Palmer, R. B. Petre, J. L. Porter, R. T. Shelton, T. L. Thomas, and J. B. Worden: Proc. SPIE Optical Engineering + Applications 2012 (SPIE, 2012) 850505.
- 9 R. Lauck, M. Brandis, and B. Bromberger: IEEE Trans. Nucl. Sci. **56** (2009) 989. <https://doi.org/10.1109/TNS.2008.2009449>
- 10 K. Watanabe, Y. Arikawa, K. Yamanoi, M. Cadatal-Raduban, T. Nagai, M. Kouno, K. Sakai, T. Nazakato, T. Shimizu, N. Sarukura, M. Nakai, T. Norimatsu, H. Azechi, A. Yoshikawa, T. Murata, S. Fujino, H. Yoshida, N. Izumi, N. Satoh, and H. Kan: J. Cryst. Growth **362** (2013) 288. <https://doi.org/10.1016/j.jcrysgro.2011.11.092>
- 11 T. Shimaoka, J. H. Kaneko, Y. Arikawa, M. Isobe, Y. Sato, M. Tsubota, T. Nagai, S. Kojima, Y. Abe, S. Sakata, S. Fujioka, M. Nakai, H. Shiraga, H. Azechi, A. Chayahara, H. Umezawa, and S. Shikata: Rev. Sci. Instrum. **86** (2015) 053503. <https://doi.org/10.1063/1.4921482>
- 12 Y. Mokuno, A. Chayahara, and H. Yamada: Diam. Relat. Mater. **17** (2008) 415. <https://doi.org/10.1016/j.diamond.2007.12.058>

- 13 T. Shimaoka, J. H. Kaneko, M. Tsubota, H. Shimmyo, H. Watanabe, A. Chayahara, H. Umezawa, and S. Shikata: *Euro. Phys. Lett.* **113** (2016) 62001. <https://doi.org/10.1209/0295-5075/113/62001>
- 14 V. Yu. Glebov, C. Stoeckl, T. C. Sangster, S. Roberts, R. A. Lerche, and G. J. Schmid: *IEEE Trans. Plasma Sci.* **33** (2005) 70. <https://doi.org/10.1109/TPS.2004.841171>
- 15 H. Shiraga, S. Fujioka, M. Nakai, T. Watari, H. Nakamura, Y. Arikawa, H. Hosoda, T. Nagai, M. Koga, H. Kikuchi, Y. Ishii, T. Sogo, K. Shigemori, H. Nishimura, Z. Zhang, M. Tanabe, S. Ohira, Y. Fujii, T. Namimoto, Y. Sakawa, O. Maegawa, T. Ozaki, K. A. Tanaka, H. Habara, T. Iwawaki, K. Shimada, H. Nagatomo, T. Johzaki, A. Sunahara, M. Murakami, H. Sakagami, T. Taguchi, T. Norimatsu, H. Homma, Y. Fujimoto, A. Iwamoto, N. Miyanaga, J. Kawanaka, T. Jitsuno, Y. Nakata, K. Tsubakimoto, K. Sueda, N. Morio, S. Matsuo, T. Kawasaki, K. Sawai, K. Tsuji, H. Murakami, T. Kanabe, K. Kondo, R. Kodama, N. Sarukura, T. Shimizu, K. Mima, and H. Azechi: *High Energy Density Phys.* **8** (2012) 227. <https://doi.org/10.1016/j.hedp.2012.03.008>

